J. Plasma Fusion Res. SERIES, Vol. 4 (2001) 131–137

Spiral Pattern Formation in a Rotating Cylindrical Plasma

TANAKA Masayoshi Y.* and KONO Mitsuo[1]
National Institute for Fusion Science, Toki, Gifu 509-5292, Japan
[1]Faculty of Policy Studies, Chuo University, Hachioji, Tokyo 192-0393, Japan

(Received: 5 December 2000 / Accepted: 27 October 2001)

Abstract

Spiral pattern formation in a rotating magnetized plasma is examined. Experimental observations are presented to show the characteristic features of spiral structure observed in an ECR plasma. To understand the experimental results, low frequency perturbations in a rotating cylindrical plasma are described using two-fluid approximation, and the eigenvalue problem is numerically solved to show the existence of spiral solutions. It is found that dissipative drift wave instability may generate spiral patterns, which well explain the experimental observations. The universal mechanism of spiral pattern formation is proposed.

Keywords:
spiral pattern, rotating plasma, drift wave, vortices

1. Introduction

Spiral patterns are commonly observed in many rotating systems such as rotating ordinary fluids, typhoon, galaxy etc. [1]. Recently, spiral patterns have been observed in magnetized plasmas; Ikehata *et al.* observed a persistent spiral structure in a gun produced plasma rotating at a supersonic speed [2], while Tanaka et al. observed a stationary spiral pattern in an ECR plasma [3], whose rotational velocity is in subsonic region. These experimental results suggest that spiral structure is a robust entity, and the underlying mechanism on spiral formation is common among many different systems.

It is easily understood that self-generation of coherent structures originates from a certain kind of instability in the system under consideration. Then, we expect that the observed spiral is a developed state of instability grown in a rotating magnetized plasma, and that eigen-mode analysis under the given boundary condition should be done as usual. However, describing spiral pattern seems to be difficult, because the locus of constant phase points in the polar coordinate system, for example spiral arms, is a function of radius r and angle θ. The radial mode is dependent on the azimuthal one, and thus the decomposition into a radial and an azimuthal modes seems to be useless. Moreover, the existence of stationary structure means that zero-eigenfrequency solution should exist, which imposes a strong limitation on the solution of unstable modes.

Then, the problems of interest in this study are whether or not such a particular solution does exist, and how it makes spiral patterns.

In this paper, we show that dissipative drift wave instability in a rotating magnetized plasma can produce a stationary spiral structure in density and potential. In the first part, the experimental results on spiral structure observed in an ECR plasma are presented, and it is shown that the observed spiral is a kind of density modulation pattern categorized into an Archimedean spiral. Then, to understand the experimental results, low frequency instabilities in a rotating magnetized plasma are described using two-fluid approximation. The linear eigenvalue problem is numerically solved to show the

*Corresponding author's e-mail: mytanaka@nifs.ac.jp

existence of spiral solutions, which well reproduce the characteristic feature of experimental observations. The universal mechanism of spiral pattern formation is proposed with a simple example, and it is concluded that spiral structure is a kind of interference pattern between azimuthal mode function and radial mode function, the latter of which becomes complex in an unstable system.

2. Experimental Results

Plasmas were produced in a cylindrical chamber with external magnetic fields, by a microwave with a frequency 2.45 GHz launched along the field line from an open end of the chamber. The magnetic field configuration was so-called a beach structure for this microwave, and the electron cyclotron resonance point was located in the middle of the chamber. An electron cyclotron wave was excited in the plasma [4], and fully absorbed before reaching the ECR point because of the large absorption coefficient. An argon gas was used in the experiment, and the electron temperature and density were 5 eV and 1×10^{12} cm^{-3} for the input power ≤ 1 kW, respectively. Stationary spiral patterns were observed in the pressure range $1 - 2 \times 10^{-2}$ torr. The size of plasma was 20 cm in diameter and 50cm in axial length.

Figure 1 shows an end view image of a spiral pattern taken by a CCD camera located at the other open end of the cylindrical chamber. This pattern doesn't move with time, when the experimental conditions are kept constant. This means that the eigenfrequency of this pattern is equal to zero. As seen in this figure, there are two winding arms, the radius of which in the polar coordinate system is proportional to the angle of rotation as shown in Fig.2. This is the characteristic feature of Archimedean spiral.

To identify what makes spiral structure, we carried out visible line image measurements (see Fig. 3). Figure

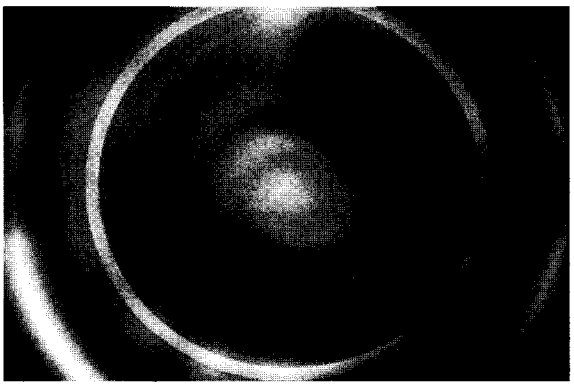

Fig. 1 End view image of spiral structure in an ECR plasma.

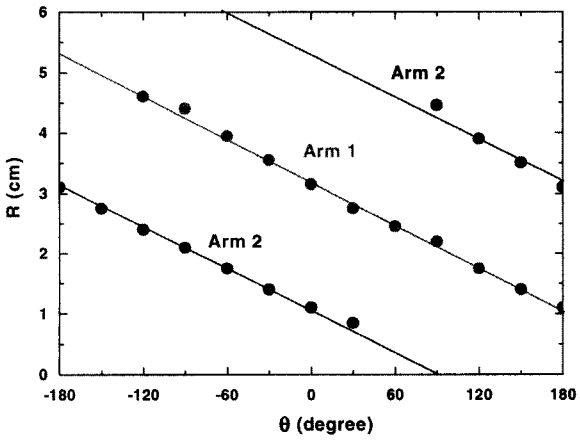

Fig. 2 Arm radius as a function of angle in polar co-ordinates.

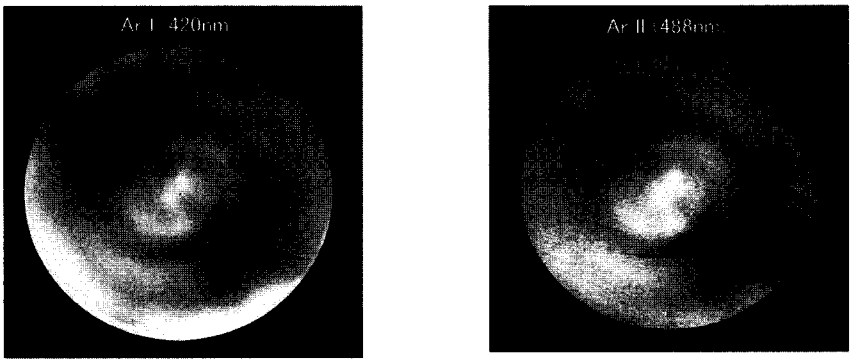

Fig. 3 Line emission image. Left: ArI (420 nm), right: ArII (488 nm).

3(a) is the gray scale image for neutral argon line ArI (420 nm), and Fig.3(b) for argon ion line ArII (488 nm). Since the electron temperature is almost constant over the whole cross section, the gray scale in Figs.3(a) and (b) are roughly proportional to $n_0 n_e$ and $n_i n_e$, respectively. The same patterns are seen in the both figures. Considering that the pattern of ArII image represents density perturbation, we can conclude that the observed spiral is a density modulation pattern.

As mentioned above, the spiral pattern doesn't move with time (stationary structure), however, the background plasma rotates around the center axis due to $\boldsymbol{E} \times \boldsymbol{B}$ drift. The plasma flow velocity was measured with a directional Langmuir probe [5], and the normalized azimuthal velocity as a function of radius is shown in Fig.4. As seen in this figure, the plasma rigidly rotates in the core region (r/a < 0.5, a: plasma radius), and then the azimuthal velocity decreases with radius in the outer region, indicating existence of shear (the direction of rotation is clockwise for Fig. 3).

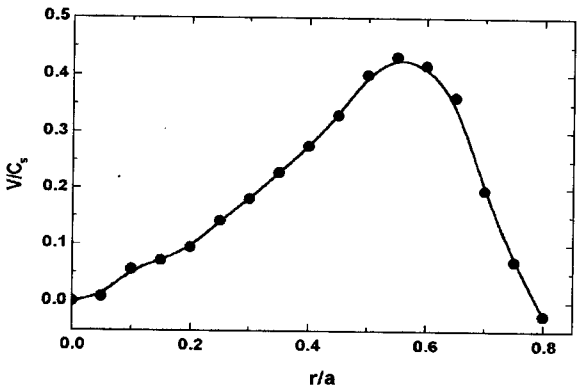

Fig. 4 Azimuthal flow velocity profile.

When the magnetic field is inverted, the polarity of rotation in spiraling into its center (refer to as polarity of spiral in the followings) changes the sign as shown in Fig. 5. It should be noted that the same patterns are seen in both figures except the polarity of spiral. Since the plasma rotates due to $\boldsymbol{E} \times \boldsymbol{B}$ drift, and this velocity changes the sign with the inversion of magnetic field $\boldsymbol{B}$, the result suggests that azimuthal rotation of plasma plays an important role in exciting the spiral density perturbation.

Here we summarize the experimental results;

(1) Spiral pattern is observed in an azimuthally rotating plasma.
(2) It is identified as a density modulation pattern and categorized into Archimedean spiral.
(3) The spiral pattern does not move with time, which means that the eigenfrequency of this structure is equal to zero in the laboratory frame.
(4) The background plasma exhibits an $\boldsymbol{E} \times \boldsymbol{B}$ rotation, and there is a shear in azimuthal velocity profile.
(5) The polarity of spiral winding changes its sign when the direction of magnetic field is inverted.

It is well known that rotating fluids excite various types of instability, and generate spatio-temporal structures such as Taylor vortices. According to the experimental observations, it is natural for us to consider electrostatic instabilities in a rotating plasma with

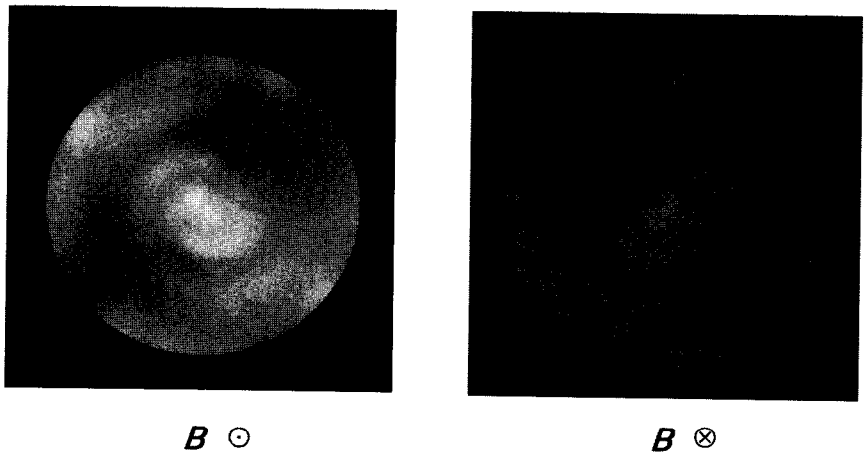

Fig. 5 Gray scale images of spiral structure. The direction of magnetic field is inverted in the right figure.

external magnetic fields.

3. Low Frequency Perturbations in a Rotating Magnetized Plasma

We consider low frequency perturbations in a rotating plasma with external magnetic fields. Special attention is paid to stationary structure and its spatial pattern, to explain the experimental observations

Low frequency perturbations in a rotating plasma is formulated using two-fluid approximation [6]. The continuity equation and the equation of motion for electrons and ions are written by ,

$$\frac{\partial n^{(\alpha)}}{\partial t} + \nabla(n^{(\alpha)} \boldsymbol{v}^{(\alpha)}) = 0 , \tag{1}$$

$$\frac{\partial \boldsymbol{v}^{(\alpha)}}{\partial t} + \boldsymbol{v}^{(\alpha)} \cdot \nabla \boldsymbol{v}^{(\alpha)} = \frac{e_\alpha}{m_\alpha}\left(-\nabla\phi + \frac{1}{c}\boldsymbol{v}^{(\alpha)} \times \boldsymbol{B}\right) - \delta_{\alpha,e}\frac{1}{n_\alpha m_\alpha}\nabla p_\alpha - \nu_\alpha \boldsymbol{v}^{(\alpha)} , \tag{2}$$

where α stands for ion or electron (i or e), $n^{(\alpha)}$ the density, and $\boldsymbol{v}^{(\alpha)}$ the velocity. We take into account dissipation due to ion-neutral and electron-neutral collisions, for which ν_α means the collision frequency. The quantity ϕ is the electrostatic potential. The ions are assumed to be cold, and the pressure gradient force is considered only for the electrons. Although the profile of unperturbed quantities, $n_0(r)$, $\boldsymbol{v}_0(r)$, and $\phi_0(r)$, are to be determined in a self-consistent manner, we here assume them, for simplicity. All the physical quantity $\boldsymbol{A}(r, z, \theta)$ is decomposed into the unperturbed part, and perturbed one, which can be expressed by the radial, azimuthal, and axial modes;

$$A(r, z, \theta) = A_0(r) + A_\ell(r) \cdot e^{\mathrm{i}(kz + \ell\theta - \omega t)} \tag{3}$$

where k is the wavenumber (complex) in axial direction, ℓ the azimuthal mode number, and ω the eigenfrequency.

The ions are subjected to $\boldsymbol{E} \times \boldsymbol{B}$ drift and the electrons to $\boldsymbol{E} \times \boldsymbol{B}$ drift and diamagnetic drift. The stationary azimuthal velocities for ions and electrons due to the unperturbed potential and density are

$$v_{0\theta}^{(\mathrm{i})} = \frac{C_\mathrm{S}^2 \Omega_\mathrm{i}}{\Omega_\mathrm{i}^2 + \nu_\mathrm{i}^2}\left[1 - \left(\frac{C_\mathrm{S}^2 \Omega_\mathrm{i}}{\Omega_\mathrm{i}^2 + \nu_\mathrm{i}^2}\right)^2 \frac{1}{r}\frac{\partial \phi_0(r)}{\partial r}\right] \tag{4}$$

$$v_{0\theta}^{(\mathrm{e})} = \frac{v_\mathrm{th}^2 \Omega_\mathrm{e}}{\Omega_\mathrm{e}^2 + \nu_\mathrm{e}^2}\frac{\partial}{\partial r}\left(\phi_0(r) - \ln n_0(r)\right) \tag{5}$$

where C_S is the ion sound velocity, v_th the electron thermal velocity. The quantities Ω_i and Ω_e are the ion cyclotron frequency and electron cyclotron frequency, respectively. The second term in ion velocity equation is the correction due to centrifugal force. Other velocity components for both ions and electrons are also obtained from Eq.(2).

Substituting these velocities for both ions and electrons into the continuity equation, linearizing and invoking the charge neutrality, we have the following equation for the perturbed potential ϕ_ℓ with a mode number ℓ :

$$\frac{\mathrm{d}^2\phi_\ell}{\mathrm{d}\xi^2} + \left[\frac{1}{\xi} + \frac{\mathrm{d}\ln n_0}{\mathrm{d}\xi}\right]\frac{\mathrm{d}\phi_\ell}{\mathrm{d}\xi} + \left[\beta(\xi) - \frac{\ell^2}{\xi^2}\right]\phi_\ell = 0, \tag{6}$$

$$\beta(\xi) = \frac{-k^2 \Omega_\mathrm{i}\Omega_\mathrm{e}}{\Gamma_\mathrm{i}(\omega)\Gamma_\mathrm{e}(\omega)}\left(1 - \frac{\ell\omega_*}{\omega - \ell\omega_\mathrm{E}}\right) - \frac{\mathrm{i}\ell}{\xi}\frac{1}{\Gamma_\mathrm{i}(\omega)}\left[\left(\omega_0^{(\mathrm{i})} + \frac{1}{a}\frac{\mathrm{d}v_{0\theta}^{(\mathrm{i})}}{\mathrm{d}\xi} + \frac{\ell\omega_\mathrm{E}^2}{\omega - \ell\omega_\mathrm{E}}\right)\frac{\mathrm{d}\ln n_0}{\mathrm{d}\xi} + \frac{\mathrm{d}\omega_0^{(\mathrm{i})}}{\mathrm{d}\xi} + \frac{1}{a}\frac{\mathrm{d}^2 v_{0\theta}^{(\mathrm{i})}}{\mathrm{d}\xi^2}\right] \tag{7}$$

where ω_E and ω_* are the angular frequency of $\boldsymbol{E} \times \boldsymbol{B}$ drift and diamagnetic drift respectively, and ξ is the normalized radius r/a. The following notations are used in Eq.(7); $\Gamma_\mathrm{i}(\omega) = \nu_\mathrm{i} - \mathrm{i}(\omega - \ell\,\omega_0^{(\mathrm{i})})$, and $\Gamma_\mathrm{e}(\omega) = \nu_\mathrm{e} - \mathrm{i}(\omega - \ell\,\omega_0^{(\mathrm{e})})$. This equation describes low frequency instabilities such as dissipative drift wave instability, centrifugal instability and Kelvin-Helmholz instability [7]. The contributions from flute modes (centrifugal instability and Kelvin-Helmholz instability) are much smaller than that of dissipative drift wave instability under the present experimental conditions, and thus we concentrate our attention to the dissipative drift wave instability (the first term of Eq.(7)).

To obtain the stationary solutions, we first fix the real part of eigenfrequency ω to zero, and numerically solve Eqs.(6) and (7) with free parameters of imaginary part of ω and wavenumber k. For this purpose, Eq.(6) is transformed into a set of ordinary differential equations, and then numerically integrated by the Runge-Kutta method, in which the boundary conditions

$$\phi_\ell = 0 \ \textit{at} \ \ \xi = 0 \ (\textit{center}), \quad \phi_\ell = 0 \ \textit{at} \ \ \xi = 1 \ (\textit{wall}) \tag{8}$$

are imposed.

Figure 6 shows the radial eigenfunction ϕ_ℓ for ℓ = 2 mode, in which the solid line indicates the real part,

and the broken line the imaginary part. It is noted that

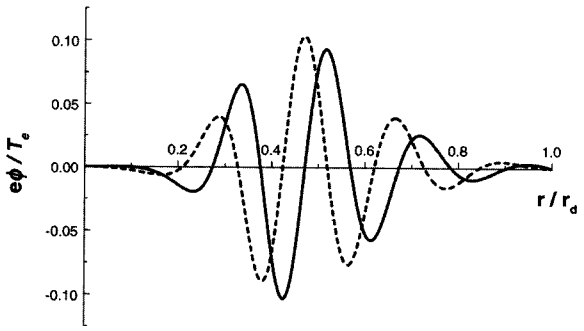

Fig. 6 Radial eigenfunction (Ref.6).

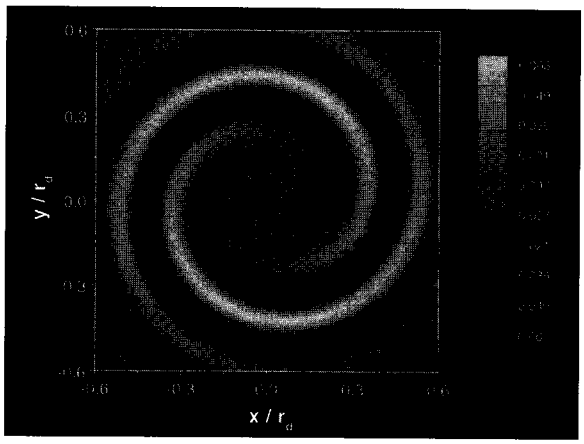

Fig. 7 Contour plot of potential (Ref.6).

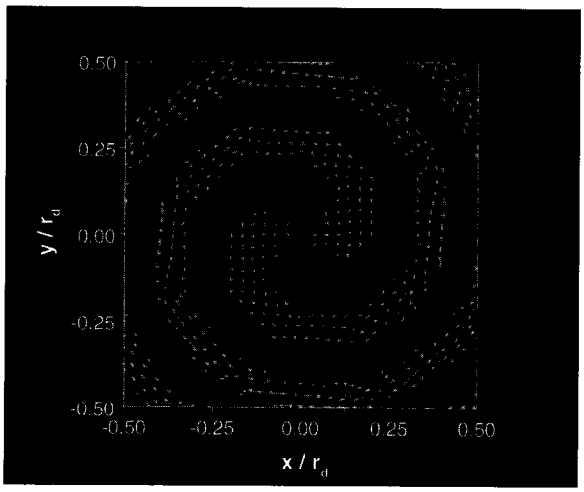

Fig. 8 Vector field plot of flow velocity associated with spiral structure (Ref.6).

the radial eigenfunction becomes a complex function, and there is a phase difference between the real and imaginary part. The phase difference plays a key role in producing spiral patterns, which will be discussed in later section.

Two-dimensional pattern is visualized by making a product of $\phi_\ell(r)\exp[i\ell\theta]$ and its contour plot for the real part, which is shown in Fig.7. A spiral pattern with two arms is clearly seen in the figure. Since the density perturbation is related to the perturbed potential, the spatial pattern of density perturbation contour is the same as Fig.7. The relation between arm radius and its angle of rotation in the polar coordinate system indicates that this spiral is an Archimedean spiral.

The vector field plot of flow velocity associated with this spiral structure is depicted in Fig.8 In this figure, each arrow is indicated by dark gray for positive radial velocity and by clear gray for negative radial velocity. It is interesting to note that the flow field associated with this spiral structure is not a sink nor a source; the plasma goes in along the clear gray arrows, reaches the center, and then goes out along the dark gray arrows, in other words, the flow vector field associated with this spiral is a circulating structure between the center and peripheral regions. This flow vector field is well explained by the $\boldsymbol{E} \times \boldsymbol{B}$ drift of the perturbed potential presented in Fig.7.

4. Universal Mechanism of Spiral Formation

We consider here the mechanism of spiral pattern formation. As already mentioned above, the existence of complex radial eigenfunction is essential in producing spiral pattern. Let us take a radial function $\phi(\beta r)$, and make a product:

$$\phi(\beta r)\cdot\exp[i\ell\theta] \tag{9}$$

where β is a parameter. When $\phi(\beta r)$ is a real function, the radial and azimuthal structures are independently determined by the radial and azimuthal functions respectively, never generating a spiral pattern. However, when $\phi(\beta r)$ becomes complex, this product is rewritten as

$$\left|\phi(\beta r)\right|\cdot\exp[i\mathrm{Arg}[\phi(\beta r)]+i\ell\theta] \tag{10}$$

The argument of radial function $\mathrm{Arg}[\phi(\beta r)]$, which is generally a function of r, is renormalized into the phase of exponential function, and produces an r-dependent phase. The condition of constant phase:

$$\mathrm{Arg}[\phi(\beta r)]+\ell\theta = const. \tag{11}$$

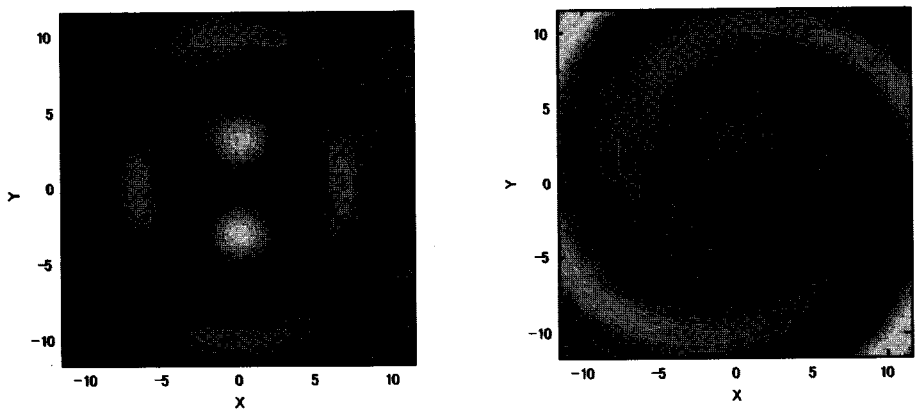

Fig. 9 Contour plot of a product of Bessel function and exponential function. (left: $\beta = 1.0$; right: $\beta = 1 + 0.25i$)

gives an $r - \theta$ relation for the locus of constant phase points, producing a spiral nature in its spatial structure. Archimedean spiral corresponds to the simplest case, in which the argument $Arg[\phi(\beta r)]$ is proportional to r.

We give here a simple example. Let us take a product of Bessel function and exponential function $J(\beta r)\cdot e^{i\ell\theta}$ ($\ell = 2$). When the parameter β is real, the azimuthal pattern produced by this product is completely determined by the exponential function, as seen in Fig.9(a). However, when β becomes complex, an "interference" between radial and azimuthal mode functions takes place, and the contour plot of this product generates a spiral pattern as shown in Fig.9(b). It is emphasized here that we don't assume any specific physical situations so far. Therefore, this scenario on spiral pattern formation may be a common mechanism underlying in many other systems [8,9].

To give the physical meaning of complex radial eigenfunction, we return to Eq.(6). When β in Eq.(6) is real, the radial eigenfunction becomes a real function. A complex radial function occurs only when β is complex. Noting that the complex β is due to the system being unstable (dissipative drift wave instability), we can conclude that the occurrence of spiral nature is attributable to the instability. It should be pointed out that instability plays an essential role in two aspects: (i) self-generation and growth of structure, and (ii) generation of spiral nature.

The physical picture of spiral formation in the present experiment is the followings; the ions rotate azimuthally by $\boldsymbol{E} \times \boldsymbol{B}$ drift. Since the ions are much heavier than the electrons, they are subjected to centrifugal force, the rotation frequency is affected by this effective gravitational force, while the electrons are driven by both the $\boldsymbol{E} \times \boldsymbol{B}$ drift and the diamagnetic drift. The difference in azimuthal drifts between the ions and electrons induces charge separation, which cannot be fully neutralized by the electrons whose axial motions are dragged by the collisions with neutral particles. Thus drift wave instability takes place and the density modulation associated with this instability is organized in such a way that the central part rotates almost rigidly, while the outer part lags behind the central part because of the shear in azimuthal velocity profile, consequently producing a spiral structure.

Although we have reported the occurrence of stationary spiral, which is easy to find out in the experiment, the occurrence of non-stationary spiral will be more general and appears in a wide range of experimental conditions.

5. Summary

The experimental results and theoretical analysis on formation of spiral structure are presented. The spiral pattern in an ECR plasma is identified as a density modulation excited in a rotating magnetized plasma. Linear mode analysis on the low frequency instability shows the existence of stationary spiral solutions, which well reproduces the experimental observations.

Since the present analysis is a linear analysis, we cannot determine the absolute value of the amplitude of perturbed density, which should be balanced, in the course of instability development, with the higher order effects and the nonlinear effect. It is very difficult to deal with this problem for general cases. However, when the characteristic scale length in radial direction is much smaller than the axial one, these scales are separable by using the reductive perturbation method

[10]. In that case, we obtain Eq.(6) for the radial eigenfunction, and the one-dimensional Gintzburg-Landau equation for the axial eigenfunction, which permits localized solutions made from competitive effect between the dispersion, diffusion, and the nonlinearity [11]. The existence of spiral structure, which is axially localized with finite amplitude, is possible.

Spiral structure is a kind of "interference " pattern between azimuthal and radial functions of unstable systems. This simple mechanism may universally occur in other unstable systems.

References

[1] M.V. Nezlin and E.M. Snezhkin, *Rosbby Vortices, Spiral Structures, Soliton*, (Springer-Verlag, Berlin, 1993).

[2] T. Ikehata *et al.*, Phys. Rev. Lett., **81** 1853 (1998).

[3] M.Y. Tanaka *et al.*, Proceedings 1986 ICPP Conf. (Nagoya, Japan) Vol.**2**, 1650.

[4] M. Tanaka *et al.*, J. Phys. Soc. Jpn., **60** 1600 (1991).

[5] K. Nagaoka *et al.*, J. Phys. Soc. Jpn., **70** 131 (2001).

[6] M. Kono and M.Y. Tanaka, Phys. Rev. Lett., **84** 4369 (2000).

[7] A.B. Mikhailovskii, *Theory of Plasma Instabilities* (Consultants Bureau, New York, 1974), Vol.**2**, Chap.7.

[8] J.R. Penano, G. Ganguli, W.E. Amatucci, D.N. Waliker and V. Gavrishchaka, Phys. Plasmas, **5** 4377 (1998).

[9] A.T. Burke, J.E. Maggs and G.J. Morales, Phys. Rev. Lett., **84** 2000 (1451).

[10] M. Kono and M.Y. Tanaka, Physica Scripta, **T84** 47 (2000).

[11] K. Nozaki and N. Bekki, J. Phys. Soc. Jpn., **53** 1581 (1984).